



Movement Characteristics of a Vibration Actuator System for Inspection of Steel Structures

Hiroyuki Yaguchi*, Isami Abiko and Shuto Ohyama

Tohoku Gakuin University, Faculty of Engineering, 3-1, Shimizukoji, Wakabayashi, Sendai, Miyagi, 984-8588, Japan

Email: yaguchi@mail.tohoku-gakuin.ac.jp

Abstract Economic development in many parts of the world has led to the construction of large structures. In Japan in particular, the proportion of social infrastructure that is 50 years old is around 55%. So far, methods for moving mechanisms on walls have been developed, such as suction systems using permanent magnets. On the other hand, robots based on drone technology have been actively developed. However, they are large and weigh more than 5 kg. In addition, due to their susceptibility to gusty winds and thunderstorms, inspection techniques based on drone technology are not yet fully established. In this study, a new actuator system is proposed which improves on the actuator proposed by the authors and has excellent propulsion characteristics and can move in all directions. It has been shown that the propulsion characteristics of the actuator can be improved by exciting the permanent magnets of the vibration component with two electromagnets placed opposite each other in an acrylic frame. A prototype actuator system was also developed in which the actuator was coupled to two pieces of flexible silicone rubber material. Tests on the actual machine have shown that this actuator system can provide more than twice the propulsive force and control the direction of movement compared to a single actuator. The possibility of using the actuator system as a drive source for inspection robots is demonstrated in this paper.

Keywords Actuator system, Vibration, New drive source, linear and rotational movement.

1. Introduction

Economic development in many parts of the world has led to the construction of large structures. In Japan in particular, the proportion of social infrastructure that is 50 years old is around 55%. Large structures built in recent years meet seismic standards. On the other hand, social infrastructure built in the past has not yet been built to seismic standards and may collapse in the event of a disaster. In addition, the number of bridges with vehicle weight restrictions is increasing every year due to age-related damage and deterioration. Therefore, establishing inspection and maintenance methods for social infrastructure such as large bridges is one of the most important issues worldwide. However, bridges are extremely difficult to inspect due to their location. For this reason, various inspection robots have been developed to ensure worker safety and reduce costs.

So far, methods for moving mechanisms on walls have been developed, such as suction systems using permanent magnets [1, 2], attraction control systems using electromagnets [9], coupled models of permanent magnets and magnetic wheels [10, 11], vacuum systems using pumps [12-14], wind power systems using propellers [15], coupled models of suction cups and vibrations [16, 17], models using claw grippers [18-20] and models using roller [21, 22]. These inspection robots use a number of electromagnetic motors as the drive source. Most of the reduction gears and additional devices inserted between the motors and the mechanical part limit the improvement of the drive characteristics. Thus, robots with built-in electromagnetic motors increase



the weight and cannot be used for the inspection of large structures. On the other hand, robots based on drone technology have been actively developed [23-25]. However, they are large and weigh more than 5 kg. In addition, due to their susceptibility to gusty winds and thunderstorms, inspection techniques based on drone technology are not yet fully established.

The authors proposed an vibration type actuator that can move on magnetic materials with a new drive principle using electromagnetic forces and inertial forces generated by mechanical resonance [26, 27]. The prototype is smaller and lighter than existing robots and has many advantages in terms of operating efficiency and scalability. However, with this drive, the direction of motion was limited to one direction. Furthermore, although it has excellent propulsion characteristics per its own weight, the traction force is low at about 1 N.

In this study, a new actuator system is proposed which improves on the actuator proposed by the authors and has excellent propulsion characteristics and can move in all directions. It has been shown that the propulsion characteristics of the actuator can be improved by exciting the permanent magnets of the vibration component with two electromagnets placed opposite each other in an acrylic frame. A prototype actuator system was also developed in which the actuator was coupled to two pieces of flexible silicone rubber material. Tests on the actual machine have shown that this actuator system can provide more than twice the propulsive force and control the direction of movement compared to a single actuator. The possibility of using the actuator system as a drive source for inspection robots is demonstrated in this paper.

2. Structure of vibration actuator

Figure 1 shows a vibration actuator that can move on magnetic surfaces such as iron. The actuator consists of a square acrylic frame, a vibration component and primary and secondary NdFeB permanent magnets attached to the underside of the frame. These NdFeB permanent magnets are bonded to a 1mm thick natural rubber material to increase friction. Conventional actuators consist of a permanent magnet, a spring and an electromagnet for excitation [26, 27]. However, the actuator proposed in this study can excite the permanent magnet with two opposing electromagnets, which is expected to improve the propulsion characteristics. A square frame with a width of 10 mm and a side length of 65 mm was machined from acrylic material. The vibration component is in the form of an NdFeB permanent magnet held by two springs. Two compression coil springs with a length of 25 mm, an outer diameter of 12 mm and a spring constant of 2178 N/m were used as the spring material.

The permanent magnet is a cylindrical NdFeB, axially magnetised. Its dimensions are 12 mm in diameter and 5 mm in height. The surface magnetic flux density measured with a Teslameter was 358 mT. An electromagnet with an iron core 3.75 mm in diameter and 22 mm in length with 900 turns of 0.2 mm copper wire was used in the experiment. By applying an alternating current to the electromagnets, an excitation force could be generated in the permanent magnets to cause the vibration components to resonate. The primary NdFeB magnet attached to the bottom of the frame has a diameter of 10 mm and a thickness of 2 mm; the secondary permanent magnet has a diameter of 6 mm and a thickness of 1 mm. The primary NdFeB permanent magnet mounted to hold the actuator to the magnet material. The secondary permanent magnet was mounted at 22 mm from the end of the frame to ensure stable linear motion of the actuator. The actuator has a height of 70 mm, a length of 70 mm and width of 10 mm and a total mass of 45.6 g.

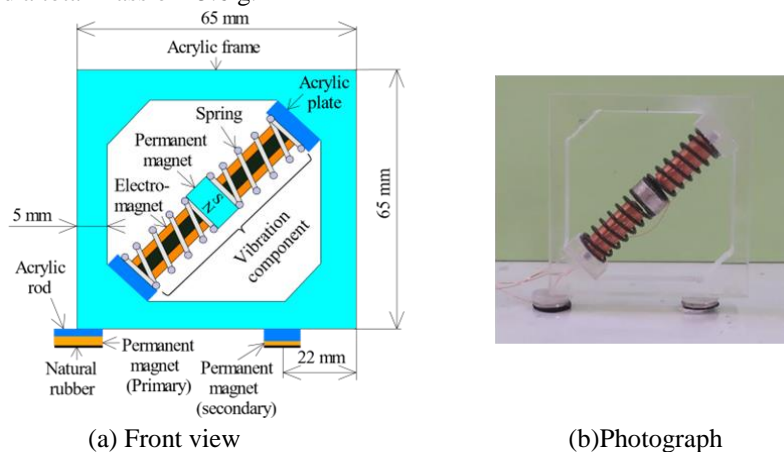


Figure 1: Structure of vibration actuator.



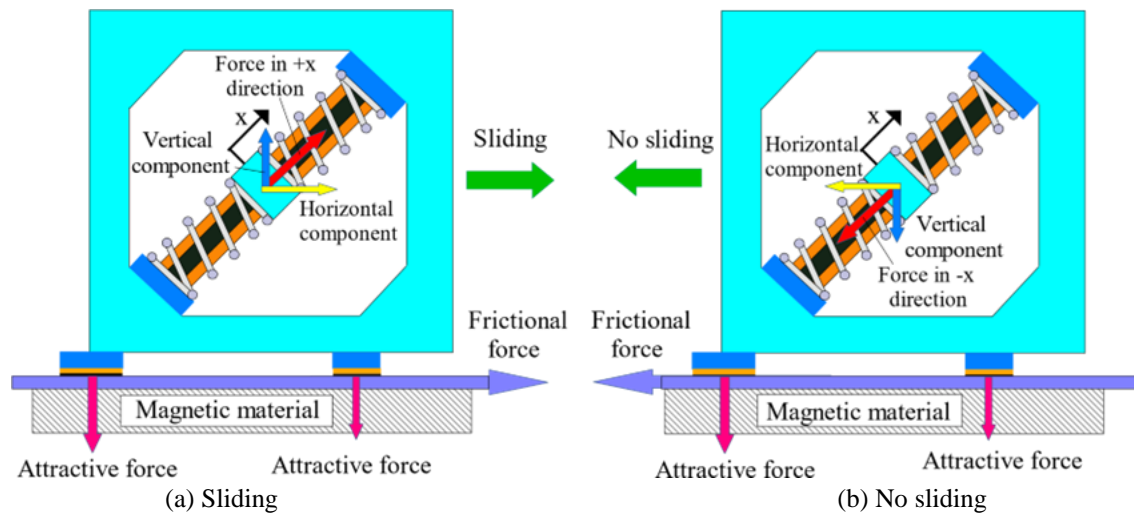


Figure 2: Principle of locomotion.

As shown in Figure 2, when the actuator is placed on a magnetic material, the holding section of the actuator is attracted by two permanent magnets attached to the support. Being held by the attraction of the permanent magnets, the vibration component vibrates and generates an alternating force on the holding section.

The displacement coordinates of the permanent magnets forming the vibration component are x . The vibration components mounted at a 45 degrees angle generate forces in the direction of 45 degrees during vibration. This force can be split into vertical and horizontal forces. The vertical force component changes the frictional force of the support section. As shown in Figure 2(a), if the vibration component is displaced in the $+x$ direction, the frictional force is reduced by the vertical component force and the actuator can move in the direction shown in Figure 2(a). On the other hand, if the vibration component is displaced in the $-x$ direction, the frictional force increases due to the vertical partial force and the actuator cannot move in the direction shown in Figure 2(b). Thus, in a vibration cycle, the actuator moves in the direction in which the vibration component is tilted, repeatedly moving and stopping as shown in Figure 2.

3. Locomotion characteristics of vibration actuator

In the experiment, an iron plate (width: 350 mm, length: 350 mm, thickness: 60 mm) was used as the target magnetic material. The vibration component in the actuator was driven at the resonance frequency of 130 Hz using a function signal generator and an amplifier. During the measurement, the coefficient of friction was 0.8. An experimental test was conducted using the apparatus shown in Figure 3. The holding force of the primary permanent magnet attached to the bottom of the frame is 3.4 N and that of the secondary permanent magnet is 2.9 N. The attractive force was measured by attracting the actuator to the iron rail and pulling the actuator body by using a spring balance. This actuator is capable of flat plane, ceiling and wall climbing motions.

Figure 4 shows the relationship between the input current to the respective electromagnets inserted in the vibration component and the linear speed for the flat plane, ceiling and vertical planes. The amplifier and the two electromagnets were connected in parallel. In the figures, the solid lines show the results of the measurements approximated by the method of least squares. Subsequently, the curves in all figures show the results of the least squares approximation of the measurements. The linear speed of the actuator increases in all planes as the input current increases. In the ceiling plane, the speed increases more than in the flat plane because gravity reduces the attraction of the permanent magnets in the holding area. In addition, the decrease in speed in the vertical plane is due to the greater effect of the weight of the actuator on the linear speed.

Figure 5 shows the relationship between the load mass on the actuator and the vertical upward speed as the input current to the respective electromagnets is varied. The load mass on the actuator was mounted by means of a thread. The figure shows that the vertical up speed decreases as the load mass increases. When a current of 0.35A is applied to the electromagnets of this actuator, the actuator can pull an additional mass of 180g, which is four times its own weight.



The above results show that the actuator has high propulsive characteristics, as demonstrated by the tests on the actual machine. However, the actuator can only move in one direction and the direction of movement cannot be controlled. Further improvement of the propulsion characteristics is necessary as various sensors need to be mounted to inspect the structure.

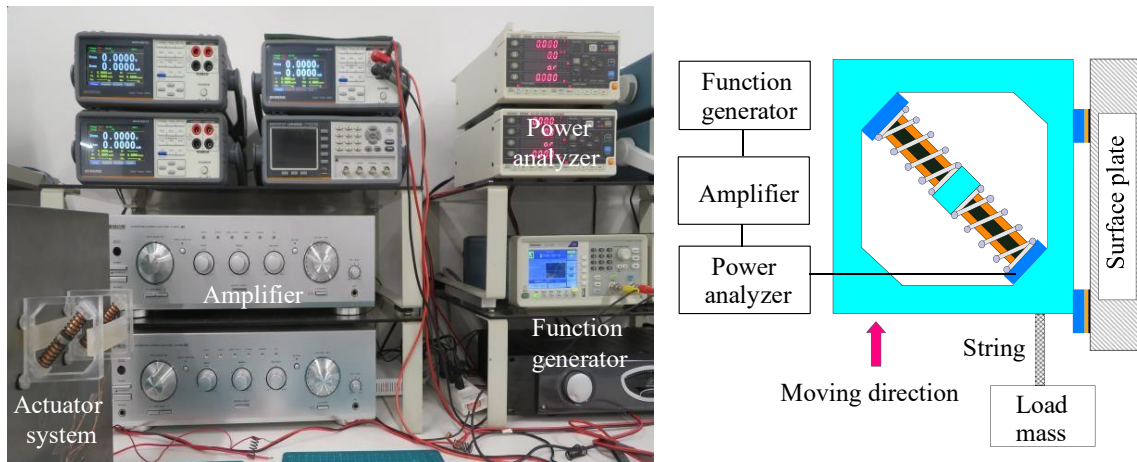


Figure 3: Experimental apparatus.

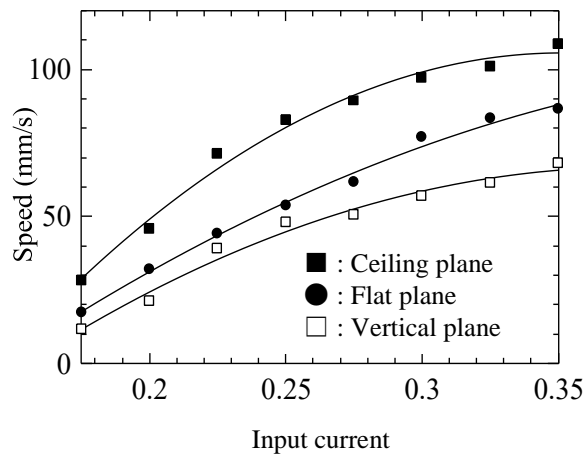


Figure 4: Relationship between input current and speed.

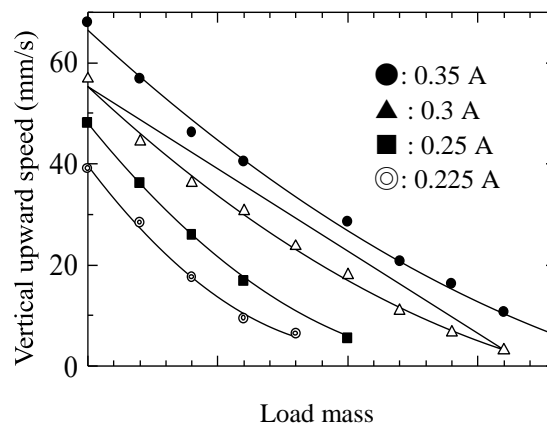


Figure 5: Relationship between load mass and vertical upward speed.

4. Locomotion characteristics of vibration actuator system

In order to change the direction of movement and to improve the drive characteristics, a new actuator system was proposed in which the actuators shown above were connected in parallel. In Figure 6, actuators A and B



have the same parameters and have been adjusted to obtain the same driving characteristics at the same resonant frequency. Two flexible silicone rubbers with a thickness of 5 mm, a width of 20 mm, a length of 90 mm and a mass of 10 g were used to connect actuators A and B. When actuators A and B were connected, the actuator system could not operate due to vibration interference when both were connected with rigid materials such as acrylic. After trial and error, the dimensions and length of the silicone rubber described above were determined. The actuator system has a length of 90 mm, a width of 90 mm and a height of 70 mm and has a total mass of 110 g.

Figure 7 shows the relationship between the input current to the respective electromagnets inserted in the vibration component and the linear speed in the prototype actuator system, for the flat plane, ceiling and vertical planes. In this case, the amplifier and all four electromagnets were connected in parallel. As the input current increases, the linear speed of the actuator system increases in all planes. The speed of the actuator system was lower than that of the actuator alone in all planes. This may be due to the increase in total mass due to the addition of the silicone rubber material and vibration disturbance.

Figure 8(a) shows the relationship between the load mass on the actuator system and the vertical upward speed as the input current to the respective electromagnets is varied. The figure shows that the vertical upward

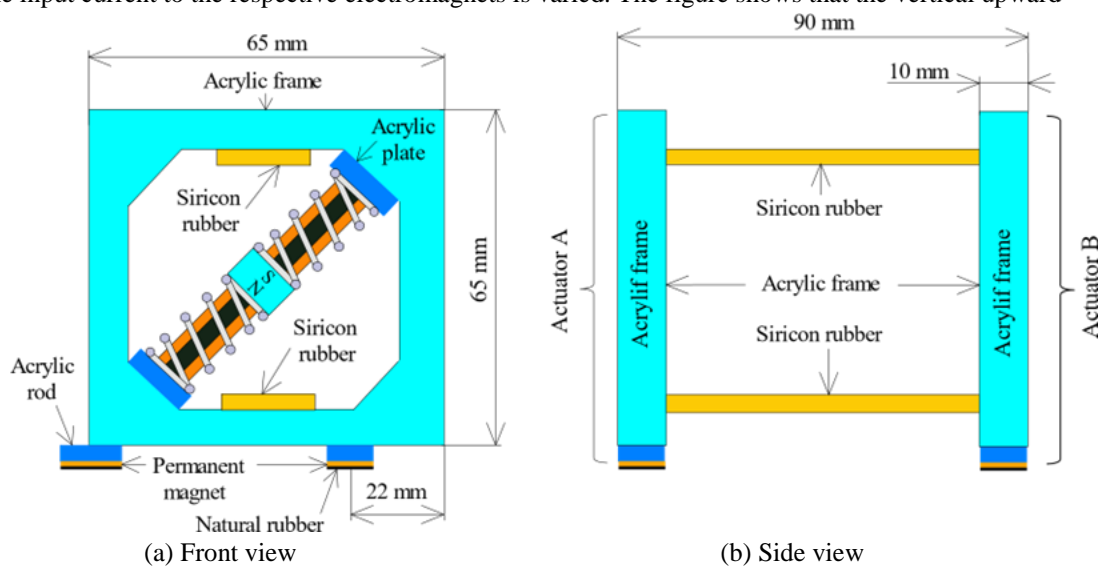


Figure 6: Structure of vibration type actuator system.

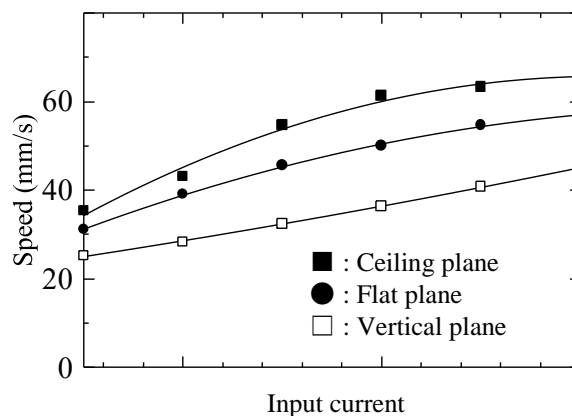


Figure 7: Relationship between input current and speed.



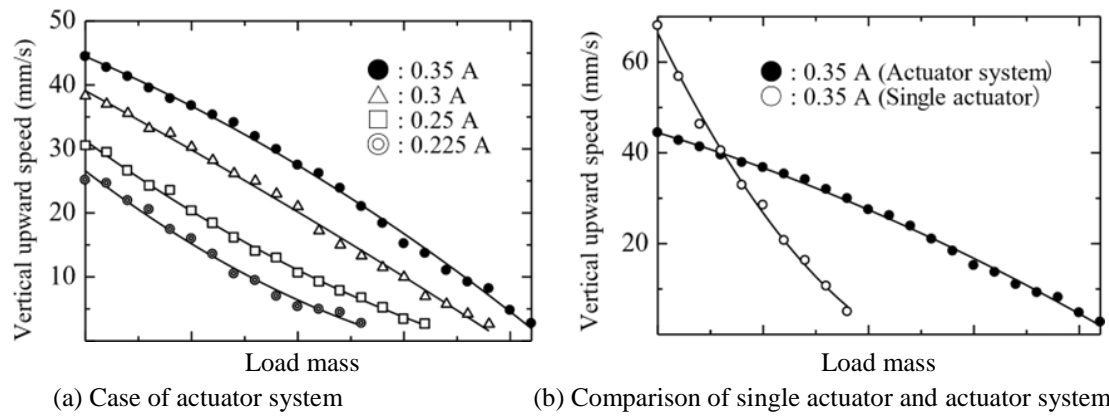


Figure 8: Relationship between load mass and vertical upward speed.

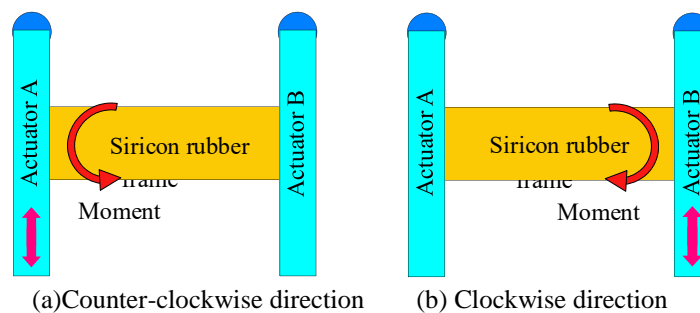


Figure 9: Principle of turning.

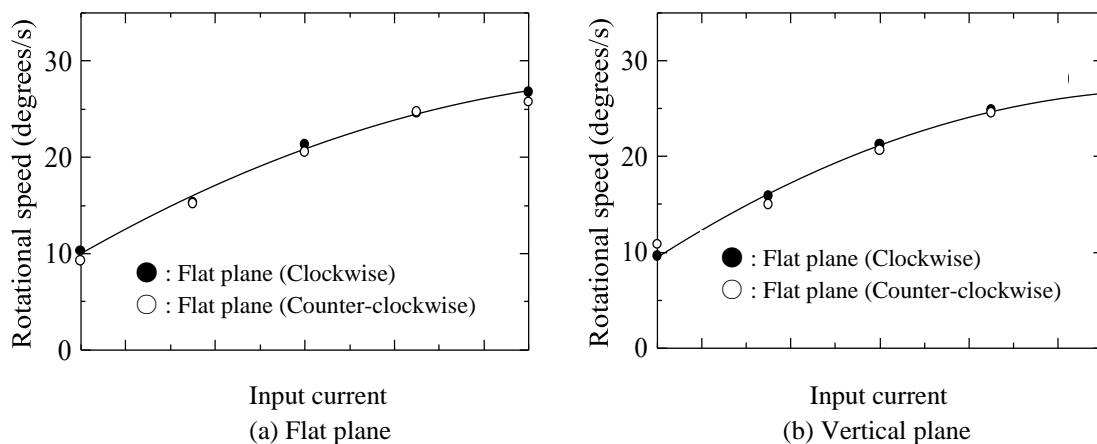


Figure 10: Turning speed of the actuator system.

speed decreases as the load mass increases. When a current of 0.35 A is applied to an electromagnet, this actuator system can pull an additional mass of 420 g, which is more than four times its own weight.

Figure 8(b) compares the drive characteristics for the single actuator and the actuator system when a current of 0.35 A is applied to each electromagnet. Essentially, at zero load mass, the movement speeds of both systems are the same for the same input current. Also, at the same input current, the pulling force of the actuator system is twice that of the single actuator. However, the speed and maximum traction force at mass 0 differed between the two figures. This is due to the fact that at low loads the actuator system was affected by vibration perturbations. On the other hand, at high loads, the silicone rubber joint stabilised the motion of the actuator system.

Finally, the rotational characteristics of the actuator system were investigated. In this actuator system, when actuator A is moved and actuator B is stationary, as shown in Figure 9(a), a moment is generated in the support section of the stationary actuator to rotate the actuator system counter-clockwise. On the other hand, when actuator B is moved, as shown in Figure 9(b), the system can be rotated clockwise.

Figure 10(a) shows the results when the actuator system is set in the flat plane and the relationship between the input current to each electromagnet and the speed is rotated clockwise and anti-clockwise with actuators A and B respectively operated. On the other hand, Figure 10(b) shows the relationship between the input current to each electromagnet and the speed when the actuator system is set in the vertical plane and actuators A and B are operated respectively. The results of both figures show that the rotational speed increases almost linearly with increasing input current. In addition, in the two planes, almost the same rotational speeds can be achieved in both clockwise and counter-clockwise directions. It was also shown that the measurement results in the flat and vertical planes were almost identical. This is due to the fact that when the attraction force is relatively high, as in this actuator system, there is no difference between the measurement results in the horizontal and vertical planes when the actuators are installed in the vertical plane, because the moments due to gravity of actuators A and B cancel each other.

5. Conclusion

A new vibration actuator was proposed with a frame structure that could excite a permanent magnet with two electromagnets. Furthermore, an actuator system was proposed in which two actuators of identical dimensions were connected by a flexible silicone rubber material. The actuator system was shown to be capable of movement in flat plane, ceiling and vertical planes. The movement speed of the actuators can be varied arbitrarily by changing the input current to the electromagnets.

In the case of a single actuator, if a current of 0.35 A is applied to an electromagnet, it can move at a speed of 5 mm/s while pulling an additional mass of 180 g. On the other hand, in the case of the actuator system, if a current of 0.35 A is applied to an electromagnet, it can move at a speed of 2.7 mm/s while pulling a mass of 420 g. This paper has shown that the method of bonding flexible silicone rubber materials can stabilise the movement of the actuators while reducing vibration interference between the actuators. A method has also been proposed to rotate the actuator system by generating a moment at the fulcrum of the stationary actuator by operating the actuator on one side in the actuator system. By applying a current of 0.25 A to an electromagnet, the actuator system can be rotated at a speed of 27 degrees/sec.

The rotation speed is the same in the flat and vertical planes, so the direction of movement can be controlled in all directions. In the future, the method of excitation of the vibration component should be investigated to further improve the drive characteristics.

References

- [1]. Shen, W., Gu, J., & Shen, Y. (2011). Permanent Magnetic System Design for the Wall-Climbing Robot. in Proc., IEEE International Conference on Mechatronics & Automation, 2078-2083.
- [2]. Lee, G., Parl, J., Kim, H., & Seo, W. (2011). Wall Climbing Robots with Track-wheel Mechanism. in Proc., IEEE International Conference on Machine Learning and Computing, 334-337.
- [3]. Fukuda, T., Matuura, H., Arai, F., Nishibori, K., Sakauchi, H., & Yoshi, N. (1992). A Study on Wall Surface Mobile Robots. *Trans. Japan Soc. Mec. Eng.*, 58(5), 286-293.
- [4]. Kawasaki, S., & Kikuchi, K. (2014). Development of a Small Legged Wall Climbing Robot with Passive Suction Cups. in Proc., International Conference on Design engineering and science, 112-116.
- [5]. Yoshida, Y., & Ma, S. (2011). A Wall-Climbing Robot without any Active Suction Mechanisms. in Proc., IEEE International Conference on Robotics and Biomimetics, 2014-2019.
- [6]. Miyake, T., Ishihara, H., & Yoshimura, M. (2007). Basic Studies on Wet Adhesion System for Wall Climbing Robot. in Proc., IEEE/RSJ International Conference on Intelligent Robots and Systems, 1920-1925.
- [7]. Apostolescu, T., Udrea, C., Duminica, D., Ionascu, G., Bogatu, L., & Cartal, L. (2011). Development of a Climbing Robot with Vacuum Attachment Cups. in Proc., International Conference On Innovations, Recent Trends And Challenges In Mechatronics, 258-267.
- [8]. Akhtaruzzaman, M., Samsuddin, M., Umar, N., & Rahman, M. (2009). Design and Development of a Wall Climbing Robot and its Control System. in Proc., International Conference on Computer and Information Technology, 309-313.



- [9]. Suzuki, M., & Hirose, S., (2010). Proposal of Swarm Type Wall Climbing Robot System Anchor Climber and Development of Adhering Mobile Units. *The Robotics Society of Japan*, 28(5), 614-623.
- [10]. Khirade, N., Sanghi, R., & Tidke, D. (2014). Magnetic Wall Climbing Devices - A Review. in *Proc., International Conference on Advances in Engineering & Technology*, 55-59.
- [11]. Kim, J., Park, S., Kim, J., & Lee, J. (2010). Design and Experimental Implementation of Easily Detachable Permanent Magnet Reluctance Wheel for Wall-Climbing Mobile Robot. *Journal of Magnetics*, 15(3), 128-131.
- [12]. Kim, H., Kim, D., Yang, H., Lee, K., Seo, K., Chang, D., & Kim, J. (2008). Development of a wallclimbing robot using a tracked wheel mechanism. *Journal of Mechanical Science and Technology*, 22, 1490-1498.
- [13]. Subramanyam, A., Mallikarjuna, Y., Suneel, S., & Kumar, L. (2011). Design and Development of a Climbing Robot for Several Applications. *International Journal of Advanced Computer Technology*, 3(3), 15-23.
- [14]. Panich, S. (2010). Development of a Climbing Robot with Vacuum Attachment Cups. *Journal of Computer Science*, 6(10), 1185-1188.
- [15]. Jae-Uk, S., Donghoon, K., ong-Heon, J., & Hyun, M. (2013). Micro aerial vehicle type wall-climbing robot mechanism. in *Proc., IEEE RO-MAN International Symposium on Robot and Human Interactive Communication*, 22-725.
- [16]. Wang, K., Wang, W., Li, D., Zong, D., Zhang, H., Zhang, J., & Deng, Z. (2008). Analysis of Two Vibrating Suction Methods. in *Proc., IEEE International Conference on Robotics and Biomimetics*, 1313-1319.
- [17]. Wang, W., Wang, K., Zhang, H., & Zhang, J. (2010). Internal Force Compensating Method for WallClimbing Caterpillar Robot. in *Proc., IEEE International Conference on Robotics and Automation*, 2816-2820.
- [18]. Xu, F., Wang, X., & Jiang, J. (2012). Design and Analysis of a Wall-Climbing Robot Based on a Mechanism Utilizing Hook-Like Claws. *International Journal of Advanced Robotic Systems*, 9(261), 1-12.
- [19]. Funatsu, M., Kawasaki, Y., Kawasaki, S., & Kikuchi, k. (2014). Development of cm-scale Wall Climbing Hexapod Robot with Claws. in *Proc., International Conference on Design Engineering and Science*, 101-106.
- [20]. Provancher, W., Jensen-Segal S., & Fehlberg, M. (2011). ROCR: An Energy-Efficient Dynamic WallClimbing Robot. *IEEE Transaction on Mechatronics*, 16(5), 897-906.
- [21]. Hagiwara, T., Yamamura, Y., Namima, Y., Ogami, J., & Pengfei, L.(2021). Production of Crawler Robot with Sub Crawler and Verification of Traversing Ability. *Second International Symposium on Instrumentation, Control, Artificial Intelligence, and Robotics (ICA-SYMP)*, 1 - 4.
- [22]. Kumar, S., and Arora, M.(2019). Design and Application of Crawler Robot. *6th National Conference on Advancements in Simulation and Experimental Techniques in Mechanical Engineering (NCASEme)*, 90 - 94.
- [23]. Rushood, M., Rahbar, F., Shokri, S., Selim, S., & Dweiri F. (2023). Accelerating Use of Drones and Robotics in Post-Pandemic Project Supply Chain. *Drones*, 7(5), 1 - 9.
- [24]. Mahamud, N., Muhammad, G., Shahriar, H., Khan, H., Sharmin, S., & Lisa, N. (2017). ALW drone : A New Design and Efficient Approach. in *Proc., IEEE 19th International Conference on Computer and Information Technology*, 474 - 479.
- [25]. Morita, M., Kinjo, H., Sato, S., Sulyon, T., & Anezaki ,T. (2017). Autonomous Flight Drone for Infrastructure (transmission line) Inspection. in *Proc., IEEE International Conference on Intelligent Informatics and Biomedical Sciences (ICIIBMS)*, 198-201.
- [26]. Yaguchi, H., & Sakuma, S. (2017). Vibration Actuator Capable of Movement on Magnetic Substance Based on New Motion Principle. *Journal of Vibroengineering*, 19(3), 1494 - 1508.
- [27]. Yaguchi, H., & Sakuma, S. (2015). A Novel Magnetic Actuator Capable of Free Movement on a Magnetic Substance. *IEEE Transactions on Magnetics*, 51(11), 4159 - 4162.

